Original Paper

Recent investigations of early Roman cameo glass

Part 2. X-ray fluorescence analyses induced by synchrotron radiation[1)]

Hans Mommsen, Axel Brüning, Heiko Dittmann, Anna Hein, Achim Rosenberg and Guido Sarrazin

Institut für Strahlen- und Kernphysik, Universität Bonn (Germany)

The elemental composition of 14 Roman cameo glass fragments was measured quantitatively by X-ray fluorescence analysis induced by synchrotron radiation. The study was intended to learn more about the possible manufacturing techniques of these glasses. In the white cameo decor of nine fragments all belonging to vessels a higher lead oxide concentration was detected compared to the colored body. In contrast, lead oxide is not enhanced in the remaining five fragments from cameo disks or plates. The higher concentrations may be interpreted as flux added to lower the melting temperature of the white cameo layers of the vessels, thus supporting the recent hypothesis that these cameo vessels were manufactured with the help of a mold on a turning wheel, which had not to be used for the production of cameo plates.

Neuere Untersuchungen über frührömisches Kameoglas
Teil 2. Röntgenfluoreszenzanalysen induziert mit Synchrotronstrahlung

Die Elementzusammensetzung von 14 römischen Kameo-Glasfragmenten wurde mit der Röntgenfluoreszenzanalyse induziert durch Synchrotronstrahlung quantitativ bestimmt. Diese Untersuchung hatte zum Ziel, Informationen über mögliche Herstellungstechniken dieser Gläser zu gewinnen. In den weißen Schichten von neun Fragmenten, die alle von Kameogefäßen stammen, ist ein erhöhter Bleioxidgehalt verglichen mit dem gefärbten Gefäßkörper zu finden, der in den restlichen fünf Fragmenten von Kameoplatten oder -tellern fehlt. Dieses Bleioxid kann als Flußmittelzusatz verstanden werden, um die Schmelztemperatur der weißen Schichten zu erniedrigen. Dies unterstützt eine neue Herstellungshypothese für diese Gefäße mit Hilfe eines Models auf einer Drehscheibe, die für die Produktion flacher Kameogläser nicht eingesetzt zu werden brauchte.

1. Introduction

Part 1 of this work [1] (with further references) proposed a new manufacturing technique for Roman cameo glasses. The application of this technique favors a lower melting temperature of the white cameo decor compared to the glasses of the colored body. Since the melting temperature will depend on the glass composition, a chemical analysis of the different glass layers of such Roman cameo products may support this hypothesis.

Earlier quantitative analyses of Roman cameo glass by electron microprobe analysis [2 and 3] already revealed a difference in composition. A surprisingly high PbO content of 12.0 and 22.3 wt%, respectively, was detected in the white glass of the Portland Vase and the Auldjo Jug, while the blue glass of both vessels contained almost no PbO. A following (only qualitative) XRF survey of Roman cameo glasses in the British Museum [2] distinguished two groups of the white cameo layers, those with high and those with low lead oxide concentrations. Lead oxide is well known to act as a flux [4] lowering the melting temperature. The present study aims to increase the number of cameo glass analyses and to screen quantitatively especially the PbO concentrations of Roman cameo glasses.

An analysis method used for this purpose must fulfill several requirements: since Roman cameo glasses are very rare and valuable, not even the minute sample can be taken, the method applied must be nondestructive. Because of the unknown preservation conditions of some of the pieces, they should not be brought into a vacuum to avoid corrosion layers to splinter off. The thickness of the white glass layers on the colored body is unknown. To analyze possibly thin surface layers, a surface-sensitive method is advantageous. At breaks the thickness of the layers is visible and in some cases not larger than a few tenths of a millimeter. So, to analyze a position at a break, a point analysis method is needed here.

A special mode of X-ray fluorescence (XRF) analysis serves all these purposes very well. For several years it has been studied in the archaeometry laboratory of the University of Bonn. At the ELectron Stretcher Accelerator (ELSA) of the Physical Institute, a beam of synchrotron radiation (SR) having sufficiently high intensity even at beam diameters in the tens of micrometer range is available on air to excite X-ray fluores-

Received October 21, 1996, revised manuscript February 20, 1997.

[1)] Pt. 1. Lierke, R.; Lindig M.: Cameo manufacturing technique and rotary scratches of ancient glass vessels. Glastech. Ber. Glass Sci. Technol. **70** (1997) no. 6, p. 189–197.

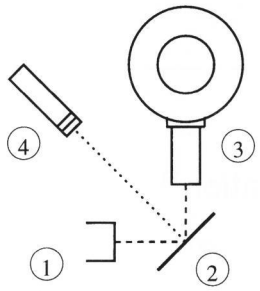

Figure 1. Schematic of the experimental setup of SYXRF, employed in Bonn; 1: incident beam, 2: sample, 3: detector, 4: laser and video camera.

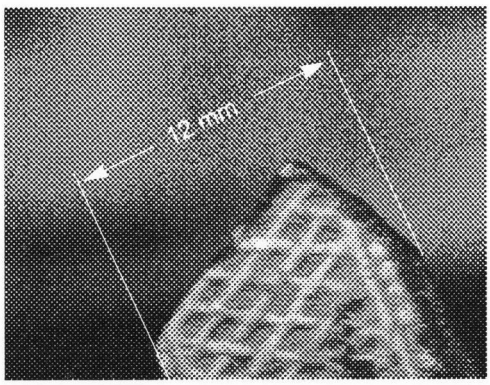

Figure 2. Video picture of measurement 12b (table 1) of fragment no. 12 (inventory number N6408a) taken during the data accumulation and stored on disk. The laser light spot visible on the rhomboid pattern marks the position analyzed.

cence radiation in any objects to be analyzed. After a short description of this method termed SYXRF and its special properties and limits, its use for and the results of the analysis of 14 cameo glass fragments from the Römisch-Germanisches Museum, Köln (Germany), will be presented and discussed. A more extended presentation of the method is given in [5].

2. Description of the SYXRF method

The properties of SYXRF are comparable to the ones of conventional XRF, except that not an X-ray tube, but the X-ray part of SR is used for excitation [6]. The white SR spectrum emitted by the electrons in ELSA circulating with an energy of usually 2.3 GeV leaves the vacuum through an aluminum window and is passed additionally through an aluminum absorber with a thickness of 1.2 mm to cut off the low-energy photons and through a remote-controlled diaphragm of variable size to collimate the beam to the wanted beam size down to the microbeam level. It is directed on the sample adjusted at a holder in such a way that its surface is inclined 45° to the beam direction as shown in figure 1. A light spot from a laser simulating the beam indicates the exact beam position chosen at the sample. It can be recorded by a video camera and stored on disk. An example of such a picture is shown in figure 2. The fluorescence radiation of the elements in the sample is measured by an energy-dispersive X-ray semiconductor detector positioned in the plane of the accelerator perpendicularly to the direction of the beam at variable distances. Because of the efficiency of the X-ray detector and the absorbing air path, X-ray lines of the elements with atomic number ≥ 19 (energy $\geq$ about 3 keV) are measurable only. The high beam intensity even at small beam sizes allows a short measuring time of a few minutes only.

To obtain quantitative results without the use of standards, the Fundamental Parameter Method (FPM) [7] is used calculating the expected fluorescence intensities from the given experimental data of the setup (experimental geometry) and known atomic physics parameters like X-ray attenuation and production cross-sections. In an iteration procedure the sample composition is varied until the calculated line intensities agree with the measured ones. As with all X-ray methods, a homogeneous sample composition has to be assumed. Since glass contains substantial amounts of elements with $Z < 19$ not detected in the fluorescence spectra, the detected elements can not be measured absolutely. In such cases elemental ratios and accordingly relative concentration values can only be determined by FPM XRF methods. Additionally, an assumption of the composition invisible to the method is needed to calculate approximatively the matrix (absorption) effects due to these light elements.

Employing an SR beam diagnostic system [8] which allows to determine the absolute number of exciting photons of SR and their energy distribution, with SYXRF not only relative, but absolute X-ray line intensities can be calculated and, therewith, absolute areal densities and concentrations of elements [5]. They sum up to the total detected part. The weight percentage of the remaining part, composed of the invisible light elements is obtained by the difference: 100 wt% − detected part. The accuracy of the quantitative results of SYXRF will depend on the reliability of the beam diagnostic system. This will be explained further discussing the data evaluation method.

Another important property of an analytical method is its sensitivity [5]. It depends on the ratio of fluorescence to background radiation. Because of the polarization of SR and the chosen measurement geometry, the background is strongly reduced. The detection limits of SYXRF at present experimental conditions are found to be in the 100 to 10 µg/g (ppm) range, but will reach values below 1 ppm, when higher electron energies of ELSA soon available can be used.

Table 1. List of Roman cameo glass fragments from the Römisch-Germanisches Museum, Köln, and positions analyzed (a = colored body, b = white layer, c = other)

fragment no. in this work	fragment and figure no. in [9]	museum invt. no.	description of cameo fragment	letter = analyzed position (decription related to figures in [9]) no. = measurement
1	1, figure 1	N1009	rim fragment of blue vessel	a1: break b1: surface, head of right woman
2	2, figure 2	N25438	body fragment of blue vessel	a1, 2: surface, left side, between spokes of wheel b1, 3: break b2: surface
3	3, figure 3	N6221	fragment of blue plate	a1, 2: surface, underneath floor b1, 2: surface, floor
4	4, figure 4	N6222	rim fragment of purple round disk with brown top layer	a1: surface, right side near rim b1: surface, left side c1: surface brown top layer
5	5, figure 5	N6223	body fragment of blue vessel	a1: break a2, 3: surface, bottom center b1: surface, center bird
6	6, figure 6	N6224	body fragment of blue plate	a1, 2, 3, 4: surface, between left leg and trunc b1, 2, 3: break
7	7, figure 7	N6225	body fragment of blue vessel	a1: break a2, 3: surface, above left below leaf b1: break b2, 3: surface
8	8, figure 8	N6226	body fragment of violet (amethyst) vessel	a1, 2: surface, bottom left side b1: surface, bottom center b2: break
9	12, figures 12 and 13	N6382a	body fragment of blue vessel (right piece in figure 12 [9])	a1, 2, 3: break b1, 2: inner surface, bottom part c1: outer surface, bottom spur
10	13, figure 15	N6382b	body fragment of blue vessel with green layer	a1, 2: break a3, 4: surface, back side b1, 2: surface, near top c1: green layer (changed color?)
11	14, figure 16	N6383b	fragment of blue plate or plaque	a1: break b1: break
12	–	N6408a	body fragment of blue vessel (5 × 7) cm^2, with rhomboid pattern	a1, 2: break b1: surface, on pattern
13	15, figure 17	N6408b	body fragment of blue glass, probably a plaque	a1, 2: break b1: break b2: surface, below eye
14	16, figure 18	N6408c	body fragment of blue vessel	a1: break a2, 3: surface, dark spot, top center b1: surface, bar, left side above head of woman

3. Sample description and measurements

Fourteen cameo glass fragments from the Römisch-Germanisches Museum in Köln (Germany) have been submitted for analysis. Except for piece no. 12, all of them have been described at length and depicted by Naumann-Steckner [9]. The exact production dates of the corresponding artefacts are not known, but can be placed in the time period 100 BC to 100 AD. Here only a short summary is repeated in table 1 together with a description of the positions analyzed.

Each piece was measured at least at two locations, a colored and a white one, with unchanged experimental conditions (electron energy 2.3 GeV, electron current 80 to 15 mA decreasing during electron beam storage time of 1 to 2 h, effective vertical electron beam size 6 mm full width at half maximum (FWHM), aluminum absorber 1.2 mm, size of diaphragm (300 × 300) μm^2, air path length to X-ray detector 3.0 cm, sensitive area 10 mm^2, energy resolution 135 eV at 5.4 keV, measuring time 300 s). If pos-

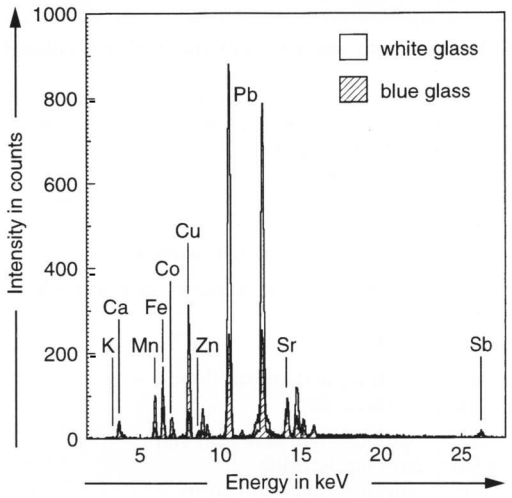

Figure 3. Spectra of a fragment no. 12 (invt, no. N6408a) put on top of each other; hatched spectrum: place on the colored glass body, nonhatched spectrum: place on the white decoration.

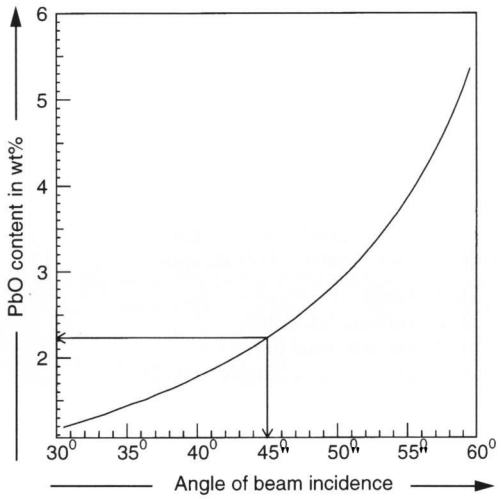

Figure 4. Dependence of calculated analysis result for PbO in the white layer of fragment no. 12 on the angle of beam incidence. A deviation of only ±5° from the assumed angle of 45° results in calculated values of 2.9 and 1.8 wt% PbO, respectively, for this fragment. This demonstrates the importance of precise angle adjustment in XRF.

sible, spots with no or the least corrosion and a flat surface have been chosen, so that the adjustment in the 45° direction to the beam was achievable with small error. As example the spectra taken from fragment no. 12 (invt. no. N6408a) at a blue and a white location are shown in figure 3 in superposition, so that the different elemental abundance especially for lead in these spectra can be seen clearly. This figure also demonstrates the low background of SYXRF.

4. Data evaluation and analytical results

The SYXRF method only allows to detect the elements visible in the spectra. As already mentioned, to evaluate reliable quantitative results for these elements with SYXRF, assumptions are necessary concerning the other nonvisible elements present in the glass. Earlier analyses of Roman cameo glass [2 and 3] determined it to be of typical soda–lime–silica type with a well-defined small range of concentrations of the main compounds (not detectable by the authors): 65 to 70 SiO_2, 16 to 17 Na_2O, 2 to 3 Al_2O_3 (data given in wt%). Assuming a similar composition of the Köln glass fragments for these compounds, approximate relative elemental compositions $Na_2O/SiO_2 = 0.25$ (Na/Si = 0.39) and $Al_2O_3/SiO_2 = 0.036$ (Al/Si = 0.041) were taken for the FPM calculations to consider the X-ray absorption effects of the invisible elements in the glass.

The analytical results will be presented both in a relative and in the absolute way because of the different error contributions in these data. The precision of the relative SYXRF depends, besides on the counting errors, on the errors given for the data entering the FPM calculations which were estimated to be about 7% for strong X-ray lines. Due to the strong absorption of the low-energy X-ray lines in air and in the glass matrix itself, the K_2O and CaO values will have larger errors. Additionally, an unknown error due to a possible wrong adjustment of the sample surface being placed at smaller or larger angles as the assumed 45° to the beam direction has to be taken into account. Due to the roughness of the fragment surfaces, deviations as large as 5° may have occurred in some cases resulting in uncertainties of up to 20 to 30%, as demonstrated by calculations depicted in figure 4 for the white layer of fragment no. 12 containing 2.2 wt% PbO. Because of this large angle-dependent error, special care was taken positioning the samples correctly.

To show the variability and to facilitate a comparison between different glass compositions, all the measurement results of the visible elements were normalized to the sum of 100 wt% and are listed in table 2 . These relative single-element concentrations have errors as quoted above.

In the last column of table 2 the absolutely measured total weight percentages of these measured elements are given. They are expected to vary from fragment to fragment, but should be the same for repeated measurements on the same glass of a fragment. Sometimes a large unexplained variability in these values is observed which, at least partly, is due to the much larger error of the absolute measurements, since a second error source additionally affects the values of the total amount of visible elements and with it all measured values likewise. It depends on the precision of the determination of the incoming photon flux hitting the sample, its spectral distribution and the geometrical factors and may reach in some cases values as large as 30%. If part of the beam misses the sample due to a misadjustment or is absorbed by a corrosion layer, too small values may be obtained. On the other hand, if the SR flux measurement done by a monitor foil misses part of the incoming intensity,

Table 2. Relative oxide concentrations of detectable elements in wt% (normalized to 100%) of the total amount visible by SYXRF given in the last column in absolute wt%. The error is estimated to be about 7%, but might be larger due an unknown error in inclination angle or due to undetected corrosion layers.

fragment no. in this work	analyzed position (letters) and no. of measurement	K_2O	CaO	MnO	Fe_2O_3	CoO	CuO	ZnO	PbO	SrO	Sb_2O_3	visible
1	a1	15	59	6.1	13.7	0.72	1.5	0.56	0.39	0.52	2.1	8.24
	b1	15	30	2.8	1.8	0.11	0.18	0.07	37.2	0.27	13	17.6
2	a1	6.2	60	8.4	13.6	1.2	1.6	0.21	0.35	0.89	7.3	4.68
	a2	16	59	2.8	5.4	1.0	12.5	0.16	4.62	0.56	6.2	8.25
	b1	8.9	21	3.2	3.1	0.089	0.23	0.086	46.5	0.32	16	36.1
	b2	9.1	24	3.9	3.9	0.17	0.29	0.079	42.0	0.35	16	16.3
	b3	5.4	66	8.95	14.4	1.2	1.6	0.16	0.22	0.61	1.8	13.3
3	a1	9.4	65	6.6	7.0	1.5	3.1	0.18	1.0	0.63	5.5	8.59
	a2	12	64	8.5	6.6	1.2	2.9	0.13	0.94	0.57	6.5	10.5
	b1	13	59	0.96	1.2	0.11	0.043	0.048	0.16	0.23	25	17.9
	b2	13	56	0.78	1.4	0.051	0.051	0.026	0.13	0.35	27	13.3
4	a1	9.2	72	12.9	4.0	0.083	0.070	0.029	0.048	0.58	1.4	11.6
	b1	11	46	1.0	1.0	0.024	0.020	0.020	0.098	0.34	40	12.7
	c1	14	73	0.21	2.9	0.047	0.025	0.025	0.058	0.67	9.4	17.0
5	a1	16	56	6.3	17.1	0.81	1.40	0.16	0.19	0.58	1.4	14.9
	a2	16	54	8.0	17.2	0.78	1.45	0.15	0.10	0.62	1.7	14.1
	a3	22	51	6.4	15.4	1.2	1.28	0.19	0.11	0.70	1.3	13.1
	b1	17	57	24	10.8	0.53	0.63	0.12	9.43	0.36	1.4	5.10
6	a1	7.6	65	5.6	17	0.96	1.8	0.55	0.19	0.65	0.75	7.71
	a2	18	58	5.9	14.3	0.99	1.7	0.46	0.052	0.49	0.79	8.75
	a3	16	59	6.5	13.4	1.0	1.4	0.39	0.20	0.51	1.6	9.24
	a4	20	56	6.0	14.1	0.96	1.7	0.39	0.058	0.46	0.37	8.36
	b1	19	69	0.90	3.0	0.22	0.48	0.14	0.46	0.54	6.1	10.4
	b2	20	44	1.3	2.6	0.095	0.31	0.059	0.67	0.37	31	11.1
	b3	17	67	3.0	4.2	0.19	0.48	0.12	0.62	0.39	7.0	19.3
7	a1	20	50	3.9	19.5	0.71	1.47	0.22	0.50	0.58	2.1	14.7
	a2	25	49	2.9	19.5	0.53	1.18	0.24	0.80	0.53	0.86	13.5
	a3	21	52	3.1	19.6	0.77	1.17	0.19	0.60	0.47	1.2	12.7
	b1	14	38	2.5	2.7	0.00	0.25	0.089	28.6	0.29	14	43.5
	b2	10	46	1.4	4.91	0.031	0.29	0.098	30.1	0.42	6.9	46.1
	b3	14	43	1.3	5.15	0.14	0.33	0.099	29.4	0.35	6.9	46.8
8	a1	15	64	14.8	4.2	0.61	0.092	0.044	0.15	0.78	0.84	10.9
	a2	18	61	14.3	4.6	0.17	0.096	0.067	0.18	0.82	0.93	11.0
	b1	9	34	2.0	2.1	0.0012	0.20	0.048	38.5	0.25	14	20.6
	b2	10	27	2.3	2.3	0.11	0.17	0.059	39.4	0.29	19	23.5
9	a1	12	73	3.5	8.7	0.54	0.95	0.090	0.12	0.58	0.86	9.56
	a2	4.5	79	4.3	8.8	0.18	0.95	0.10	0.11	0.77	1.6	4.43
	a3	32	56	2.6	6.8	0.12	0.77	0.092	0.0079	0.40	0.98	7.38
	b1	30	29	1.9	2.8	0.12	0.28	0.042	22.7	0.32	13	10.8
	b2	23	33	2.3	1.9	0.051	0.30	0.068	25.6	0.25	14	12.3
	c1	15	55	2.6	5.8	0.062	0.36	0.083	14.5	0.37	5.2	18.4
10	a1	13	62	3.1	4.6	1.0	3.69	0.14	4.69	0.57	6.4	13.7
	a2	16	56	3.0	4.8	1.0	4.50	0.21	5.96	0.75	7.8	11.2
	a3	16	59	2.8	5.5	1.0	4.37	0.16	4.66	0.56	6.3	8.16
	a4	21	52	3.1	6.8	1.1	4.61	0.22	4.93	0.65	5.4	7.40
	b1	14	17	0.89	5.2	0.16	9.28	0.16	37.8	0.24	15	7.97
	b2	12	21	1.5	2.5	0.0	10.1	0.16	34.4	0.34	18	11.7
	c1	4.7	19	0.26	0.85	0.082	19.4	0.18	50.9	0.46	4.7	38.5
11	a1	17	63	7.8	8.1	0.62	0.78	0.061	0.073	0.61	1.8	10.9
	b1	15	45	6.5	1.9	0.054	0.092	0.035	0.15	0.46	32	12.8
12	a1	12	52	7.07	6.65	1.3	5.47	0.20	3.67	0.485	12	10.3
	a2	13	49	7.4	6.77	1.3	5.09	0.22	3.26	0.51	14	13.9
	b1	9.3	57	2.1	3.1	0.21	0.99	0.084	12.3	0.47	14	18.1
13	a1	8.0	22	2.9	7.31	0.38	1.1	0.13	40.1	0.36	18	69.5
	a2	10	18	1.9	3.80	0.49	1.0	0.098	50.4	0.23	14	36.1
	b1	8.0	19	2.4	1.5	0.12	0.19	0.070	42.9	0.24	26	98.9
	b2	12	25	1.5	1.5	0.0025	0.16	0.090	35.6	0.22	24	70.0
14	a1	28	45	5.0	15.3	0.40	1.1	0.11	1.5	0.56	3.6	10.6
	a2	25	48	5.8	16.1	0.63	1.2	0.23	0.77	0.75	1.3	11.1
	a3	21	54	5.2	14.1	0.60	1.2	0.20	0.70	0.59	1.7	11.4
	b1	19	60	0.47	3.4	0.11	0.17	0.048	8.99	0.25	7.4	13.9

larger absolute amounts are calculated. Despite the large variability shown in table 2, the authors present, as far as possible, averaged absolute composition values for the colored and white glasses of the fragments in table 3. The uncertainties quoted are the spreads (root mean square deviations) or, for single measurements, the statistical errors. The measurement of the white layer of fragment no. 2 (analyzed position b, measurement no. 3 in table 2) was excluded from the averaging. It shows unexplained values which are characteristic of a blue glass: low PbO and Sb_2O_3, high Fe_2O_3 and CoO contents. Since the video picture taken during this measurement shows the laser beam to be at a white position, this result may have been caused by a misadjustment of the SR beam or a very thin surface layer of white glass. The absolute values of fragment no. 13, left out in table 3, are questionable and are only given as relative abundance in table 2. They are unusually high probably due to an error in the absolute measurement, which results in a wrong normalization to very unlikely total absolute concentrations of 70 wt% and above in three of the four cases. For the white layer of fragment no. 7 also a rather high sum of visible elements of 45 wt% is repeatedly obtained.

The remaining part made up of the invisible elements, as mentioned above, is assumed to have the given fixed relative composition of silicon, sodium, aluminum and oxygen to consider the matrix effects in an approximative way. The error due to this approximation is less important. This is demonstrated by calculations with varying Na_2O/SiO_2 content depicted in figure 5. Matrix effects due to other elements with low concentrations present in Roman glass which are not visible, like magnesium, sulfur, chlorine and phosphorus [2], are also found to be small and can be neglected.

As for conventional XRF, the analyzed depth of the sample depends mainly on the absorption of fluorescent X-rays in the glass matrix, which is strongly energy and thus Z-dependent. The authors' fundamental parameter calculations allow to determine the contributions from different depth layers. This is demonstrated by data shown in figure 6 where calculated CaK_α, PbL_α and SbK_α X-ray intensities reaching the detector are plotted (full lines) in dependence on depth below surface in beam direction. The areas below the full lines represent the intensities accumulated in the corresponding lines in the X-ray spectrum. It is seen that for the CaK_α line ($E = 3.4$ keV) a layer at a depth of 100 µm in beam direction (corresponding to a depth of $100 \times \sqrt{2}$ below surface at 45° sample inclination) contributes only about 1/5000 to the calcium line intensity emitted from a layer at the surface, whereas for antimony, due to the much higher K_α X-ray energy of $E = 26.4$ keV, a layer at a depth of 2000 µm in beam direction still contributes about 1/10 of the antimony line intensity from the surface. The broken lines represent the corresponding X-ray intensities/layer produced inside the sample. They decrease due to the attenuation of the exciting SR beam intensity. The difference between produced and detected X-ray intensities is zero for the surface layer and is explained by matrix effects inside the sample.

5. Discussion

The compositions of the cameo glass fragments from Köln measured by SYXRF agree well with the data published already [2 and 3]. The K_2O and CaO values, having large errors here, are in the expected range for Roman glass. Strontium is found to be correlated with calcium and can be assumed to have its origin in the limestone utilized by the glassmakers.

The white glass decors of the cameo fragments are generally found to have a different composition compared to the colored glasses. Antimony is known to have been added as opacifier. Its content given as weight percent of oxide (although known to be present as calcium antimonate [2]) is consistently higher in the white layers and may reach values of a few weight percent (except for fragment no. 5).

The authors' special question and the reason for the analysis concerned the PbO concentrations. Nine cameo glass fragments are found to contain appreciably higher lead concentrations in the white parts compared to the colored glass bodies. This is depicted in figure 7, where the absolute PbO concentrations for the white and the colored glasses (except for the questionable piece no. 13) are shown as bar diagram. In most cases (no. 1, 2, 7, 8, 10 (and 13?)), lead oxide comprises more than 30% of the total amount of compounds measurable by the authors (see table 2). Absolute amounts of 10 wt% PbO, about as high as reported for the Portland Vase, are detected for fragments no. 2 and 7 (table 3). It is remarkable that all the nine pieces having a high PbO content in the white layers compared to the colored glass stem from vessels, whereas the remaining five cameo fragments (no. 3, 4, 6, 11 (13?)) having low or about similar PbO content belong to plates or disks. This ascertains the findings of the British Museum. As reported by [2, p. 58], especially in cameo vessels a high percentage of high-lead white layers was found (24 out of 27 pieces), whereas in cameo plates and plaques this percentage was lower (11 out of 28 pieces). As discussed below, the difference in PbO content between the white layers of vessels and of plates or disks is now understandable assuming the new manufacturing hypothesis.

Another difference between the colored glass and the white layers is the concentration of the elements which act as coloring agents. As well known, oxides of the elements manganese, iron, cobalt and copper characterize the color, where cobalt and copper are obviously responsible for the blue coloring of the transparent glass bodies. The most intensive colorant is CoO; the other oxides like CuO and Fe_2O_3 modify the color, but these modifications are minor relative to CoO coloring [2]. In the blue glass, CoO concentrations of about 0.05 to 0.1 wt% are measured.

Table 3. Averaged absolute oxide concentrations of detectable elements in wt% (uncertainties in % in italics) adding up to the total amount listed in the last column. The remaining nondetectable elements are assumed to be Na_2O, Al_2O_3 and SiO_2 having fixed relative amounts of 19, 3 and 78 wt%, respectively.

fragment no. in this work	analyzed position	K_2O	CaO	MnO	Fe_2O_3	CoO	CuO	ZnO	PbO	SrO	Sb_2O_3	visible
1	a	1.2	4.9	0.50	1.1	0.059	0.12	0.046	0.032	0.043	0.17	8.2
		18	*4*	*4*	*3*	*10*	*3*	*7*	*7*	*4*	*22*	–
	b	2.6	5.3	0.49	0.32	0.019	0.032	0.012	6.5	0.048	2.3	17.6
		12	*7*	*6*	*6*	*12*	*10*	*14*	*0.5*	*5*	*22*	–
2	a	0.80	3.9	0.31	0.55	0.070	0.54	0.011	0.20	0.044	0.43	6.5
		91	*39*	*36*	*25*	*29*	*122*	*24*	*130*	*7*	*30*	*39*
	b	2.4	5.8	0.92	0.87	0.03	0.065	0.022	11.8	0.089	0.42	26.2
		54	*47*	*43*	*37*	*24*	*40*	*60*	*60*	*50*	*54*	*53*
3	a	1.1	6.2	0.73	0.65	0.13	0.29	0.015	0.093	0.057	0.058	9.55
		45	*16*	*32*	*12*	*7*	*8*	*21*	*12*	*8*	*32*	*14*
	b	2.0	9.0	0.14	0.20	0.013	0.0073	0.0061	0.023	0.044	4.05	15.6
		30	*27*	*41*	*14*	*76*	*27*	*67*	*40*	*12*	*19*	*21*
4	a	1.1	8.4	1.5	0.46	0.0096	0.0081	0.0034	0.0056	0.067	0.16	11.6
		30	*7*	*4*	*6*	*30*	*22*	*30*	*24*	*4*	*24*	–
	b	1.4	5.8	0.13	0.13	0.0030	0.0025	0.0025	0.012	0.043	5.1	12.7
		24	*10*	*14*	*12*	*58*	*45*	*38*	*16*	*5*	*5*	–
	c	2.4	12.4	0.036	0.49	0.0080	0.0043	0.0043	0.0099	0.11	1.6	17.0
		22	*7*	*30*	*7*	*41*	*38*	*30*	*20*	*4*	*10*	–
5	a	2.5	7.5	0.96	2.3	0.13	0.19	0.023	0.019	0.088	0.21	14.0
		19	*13*	*15*	*12*	*22*	*12*	*15*	*45*	*5*	*28*	*6*
	b	0.72	2.4	1.0	0.46	0.022	0.027	0.0051	0.40	0.015	0.059	5.1
		18	*7*	*7*	*3*	*7*	*7*	*14*	*2*	*4*	*22*	–
6	a	1.3	5.1	0.51	1.3	0.083	0.14	0.038	0.011	0.045	0.077	8.5
		45	*14*	*16*	*6*	*16*	*9*	*16*	*67*	*14*	*73*	*8*
	b	2.5	8.3	0.27	0.47	0.024	0.059	0.015	0.081	0.057	1.81	13.6
		31	*49*	*99*	*63*	*58*	*53*	*59*	*46*	*30*	*80*	*36*
7	a	3.0	6.8	0.45	2.7	0.090	0.18	0.029	0.086	0.062	0.19	13.6
		17	*7*	*24*	*9*	*20*	*21*	*21*	*14*	*35*	*57*	*7*
	b	5.8	19.3	0.79	2.0	0.027	0.13	0.043	13.4	0.16	4.22	45.5
		22	*14*	*36*	*34*	*130*	*17*	*15*	*6*	*19*	*41*	*4*
8	a	1.8	6.9	1.6	0.49	0.043	0.011	0.0061	0.018	0.088	0.096	11.0
		23	*8*	*4*	*9*	*81*	*16*	*34*	*27*	*5*	*31*	*1*
	b	2.1	6.7	0.48	0.49	0.013	0.041	0.012	8.6	0.060	3.7	22.1
		21	*10*	*21*	*18*	*139*	*11*	*30*	*12*	*19*	*32*	*9*
9	a	1.2	4.9	0.24	0.57	0.023	0.063	0.0066	0.0055	0.040	0.075	7.1
		92	*36*	*35*	*40*	*109*	*41*	*37*	*97*	*34*	*31*	*37*
	b	3.0	3.6	0.25	0.27	0.0097	0.034	0.0065	2.8	0.033	1.6	11.6
		24	*22*	*22*	*19*	*54*	*18*	*47*	*18*	*7*	*33*	*9*
	c	2.8	10.1	0.48	1.1	0.011	0.066	0.015	2.7	0.068	0.96	18.4
		18	*7*	*7*	*4*	*30*	*10*	*16*	*1*	*4*	*12*	–
10	a	1.6	5.9	0.31	0.53	0.10	0.43	0.018	0.51	0.064	0.67	10.1
		23	*36*	*31*	*15*	*28*	*21*	*29*	*32*	*31*	*39*	*29*
	b	1.3	2.0	0.13	0.35	0.0066	0.97	0.016	3.5	0.030	1.7	9.9
		28	*41*	*62*	*25*	*139*	*34*	*30*	*20*	*50*	*41*	*26*
	c	1.8	7.3	0.10	0.33	0.032	7.5	0.069	19.6	0.18	1.8	38.5
		17	*6*	*15*	*7*	*17*	*1*	*7*	*0.5*	*4*	*14*	–
11	a	1.9	6.9	0.85	0.88	0.068	0.085	0.0066	0.0080	0.066	0.20	10.9
		22	*7*	*5*	*4*	*12*	*10*	*22*	*18*	*5*	*22*	–
	b	1.9	5.8	0.83	0.24	0.0069	0.012	0.0045	0.019	0.059	4.1	12.8
		24	*10*	*6*	*9*	*41*	*22*	*29*	*14*	*5*	*6*	–
12	a	1.5	6.1	0.87	0.81	0.16	0.64	0.026	0.42	0.061	1.6	12.1
		30	*16*	*22*	*23*	*23*	*17*	*28*	*12*	*25*	*32*	*21*
	b	1.7	10.3	0.38	0.56	0.038	0.18	0.015	2.2	0.085	2.5	18.1
		27	*7*	*9*	*6*	*19*	*6*	*18*	*1*	*5*	*10*	–
14	a	2.7	5.4	0.59	1.7	0.060	0.13	0.020	0.11	0.070	*0.24*	11.0
		19	*15*	*13*	*8*	*28*	*16*	*41*	*18*	*18*	*57*	*4*
	b	2.6	8.3	0.065	0.47	0.015	0.024	0.0067	1.2	0.035	1.0	13.9
		13	*6*	*17*	*5*	*22*	*13*	*20*	*1*	*6*	*10*	–

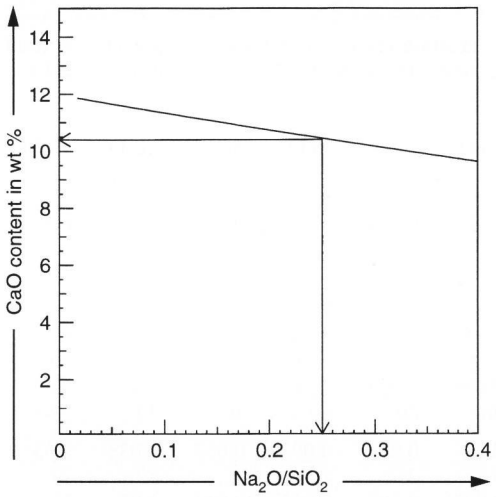

Figure 5. Variation of calculated CaO concentration in fragment no. 12 by changing the assumed Na_2O/SiO_2 concentration ratio of 0.25 in the glass matrix.

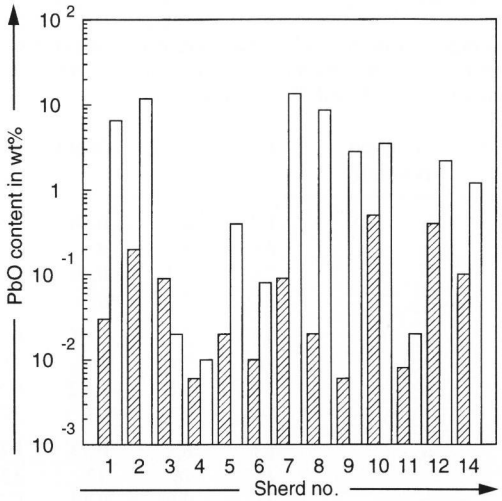

Figure 7. Content of PbO in the colored (hatched) and in the white glass (nonhatched) layers in wt% (without fragment no. 13). The nine fragments belonging to glass vessels have a higher PbO concentration in the white decors.

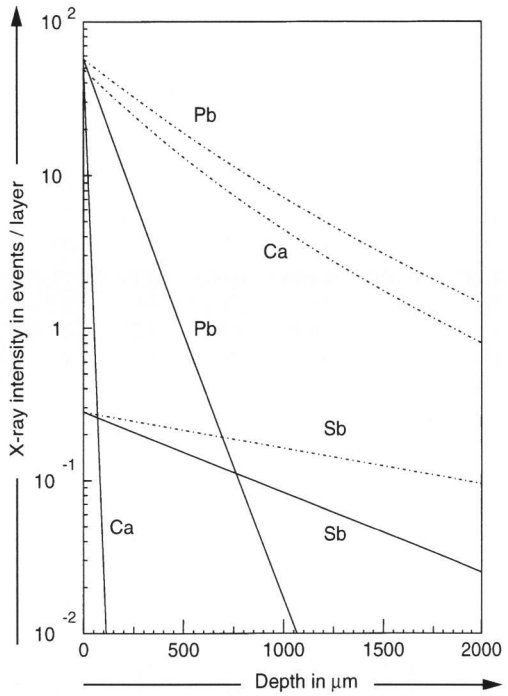

Figure 6. Calculated depth dependence of relative X-ray intensities of elements calcium, lead and antimony produced inside the white layer of fragment no. 12 (dashed curves) and of emitted part (full curves) in direction of and summed up by the X-ray detector per sample layer of 1.4 µm for excitation with the white SR beam at 2.3 GeV electron energy in ELSA (assumed density of glass 2.5 g/cm^3).

The observation [2] that a high content of manganese oxide relative to that of iron gives the glass a dark red or violet color is ascertained, too. The purple fragment no. 4 and the violet one no. 8 are found to have the highest MnO values encountered of about 1.5 and only about 0.5 wt% iron oxide. The third top layer of fragment no. 4 above the white glass layer, a transparent brown glass, does not show any unusual values. The second white layer on the back of fragment no. 9 (measurement 9c, table 3) has a different composition than the white layer of the front. An unexplained green layer above the corroded white layer of fragment no. 10 shows besides 20 wt% PbO a high CuO concentration of 7.5 wt% (measurement 10c). This makes a change of color by a copper corrosion product as mentioned by [9] very probable.

To summarize, the results of the present analysis not only ascertain the former findings, but also strongly support the new assumption that early Roman cameo glass has not been cut but molded [1]. This may be concluded from the measured higher lead content of the white cameo glass layers compared to the dark colored body glasses especially in cameo glass vessels, since an addition of PbO acts as a flux by lowering the melting temperature. According to the new manufacturing hypothesis, the white glass is deposited as a powder slurry or cameo enamel in the cavities of a mold (master negative) and fused by the heat of the glowing hot body glass which is pressed into the mold. For a fast and even distribution of the hot glass and of the additional pressure the mold is assumed to have been positioned on a turning or potter's wheel during this procedure. An addition of PbO to lower the melting temperature of the white glass slurry in the mold seems indeed to have been advantageous especially for vessels produced on a turning wheel by this technique. For plates, the lowering of the melting temperature of the white cameo glass was not needed or not so important since a turning mold was not required here and the glass powder could easily be pre-fused before the hot body glass was pressed on top. A higher PbO content should have been found

in plates too if the reason for this addition had been a better cutting property of such glasses as mentioned in [2].

*

This work has been funded partly by the Bundesminister für Bildung, Wissenschaft, Forschung und Technologie, Bonn, under contract No. 03 MN9BON and by the Deutsche Forschungsgemeinschaft (DFG), Bonn-Bad Godesberg.

6. References

[1] Lierke, R.; Lindig, M.: Recent investigations of early Roman cameo glass. Pt. 1. Cameo manufacturing technique and rotary scratches of ancient glass vessels. Glastech. Ber. Glass Sci. Technol. **70** (1997) no. 6, p. 189–197.

[2] Bimson, M.; Freestone, I. C.: An analytical study of the relationship between the Portland Vase and other Roman cameo glasses. J. Glass Stud. **25** (1983) p. 55–64.

[3] Freestone, I. C.: Recent research on the Portland Vase. Pt. 2. Studies of the Portland Vase. J. Glass Stud. **32** (1990) p. 103–107.

[4] Römpp, H.: Glas. In: Chemie Lexikon. 4th ed. Stuttgart: Franckh, 1958.

[5] Heimermann, D.: Quantitative Röntgenfluoreszenzanalyse mit Synchrotronstrahlung. Univ. Bonn, PhD thesis 1995.

[6] Pantenburg, F. J.; Beier, T.; Hennrich, F. et al.: The fundamental parameter method applied to X-ray fluorescence analysis with synchrotron radiation. Nucl. Instr. Meth. Phys. Res. **B68** (1992) p. 125–132.

[7] Sparks, C. J.: Quantitative X-ray fluorescent analysis using fundamental parameters. Adv. X-ray Anal. **19** (1976) p. 19–52.

[8] Heimermann, D.; Beier, T.; Dittmann, H. et al.: A monitor for the spectral distribution of white synchrotron radiation. Naturwissenschaften **81** (1994) p. 551–552.

[9] Naumann-Steckner, F.: Vidi tunc adnumerari unius scyphi fracta membra. Kameoglas-Fragmente im Römisch-Germanischen Museum Köln. Kölner Jb. Vor- Frühgesch. **22** (1989) p. 73–86.

0797P003

Address of the authors:

H. Mommsen, A. Brüning, H. Dittmann, A. Hein, A. Rosenberg, G. Sarrazin
Institut für Strahlen- und Kernphysik der Universität Bonn
Nußallee 14–16, D-53115 Bonn